Charge equilibrium of a laser-generated carbon-ion beam in warm dense matter

Gauthier, M., Chen, S. N., Levy, A., Audebert, P., Blancard, C., Ceccotti, T., ... Fuchs, J. (2013). Charge equilibrium of a laser-generated carbon-ion beam in warm dense matter. Physical Review Letters, 110(13), [135003]. DOI: 10.1103/PhysRevLett.110.135003

Published in:
Physical Review Letters

Document Version:
Publisher's PDF, also known as Version of record

Charge Equilibrium of a Laser-Generated Carbon-Ion Beam in Warm Dense Matter

M. Gauthier,[1,2] S. N. Chen,[1] A. Levy,[1] P. Audebert,[1] C. Blancard,[2] T. Ceccotti,[3] M. Cerchez,[4] D. Doria,[5] V. Floquet,[3] E. Lamour,[6] C. Peth,[4] L. Romagnani,[1] J.-P. Rozet,[6] M. Scheinder,[7] R. Shepherd,[7] T. Toncian,[4] D. Vernhet,[6] O. Willi,[4] M. Borghesi,[5,8] G. Faussurier,[2] and J. Fuchs[1,*]

[1]*LULI, École Polytechnique, CNRS, CEA, UPMC Université Paris 6, Route de Saclay, 91128 Palaiseau, France*
[2]*CEA, DAM, DIF, 91297 Arpajon, France*
[3]*Service des Photons, Atomes et Molécules, CEA, DSM/IRAMIS, CEN Saclay, 91191 Gif sur Yvette, France*
[4]*Heinrich Heine Universität Düsseldorf, D-40225 Düsseldorf, Germany*
[5]*School of Mathematics and Physics, The Queen's University Belfast, Belfast BT7 1NN, Northern Ireland, United Kingdom*
[6]*Institut des NanoSciences de Paris (INSP), UPMC Université Paris 6, CNRS, F-75005, Paris, France*
[7]*Lawrence Livermore National Laboratory, Livermore, California 94551, USA*
[8]*Institute of Physics of the ASCR, ELI-Beamlines Project, Na Slovance 2, 18221 Prague, Czech Republic*

(Received 5 June 2012; published 28 March 2013)

Using ion carbon beams generated by high intensity short pulse lasers we perform measurements of single shot mean charge equilibration in cold or isochorically heated solid density aluminum matter. We demonstrate that plasma effects in such matter heated up to 1 eV do not significantly impact the equilibration of carbon ions with energies 0.045–0.5 MeV/nucleon. Furthermore, these measurements allow for a first evaluation of semiempirical formulas or *ab initio* models that are being used to predict the mean of the equilibrium charge state distribution for light ions passing through warm dense matter.

DOI: 10.1103/PhysRevLett.110.135003 PACS numbers: 52.38.Kd, 34.50.Bw, 34.70.+e, 52.50.Gj

The understanding of the physical processes involved in the interaction of ion beams in warm dense matter (WDM) (i.e., plasmas characterized by temperatures ≥ 1 eV and densities near solid) is fundamental for condensed matter, solid-state physics, fusion sciences, and astrophysical phenomena [1]. More specifically, ion stopping power and charge equilibrium in WDM are highly relevant for inertial confinement fusion (ICF) [2].

For cold matter, different theoretical approaches have been developed to describe the average charge state of an ion beam passing through matter and extended descriptions of these models are discussed in Ref. [3]. Giving here only a brief overview, two different parameters are commonly used: namely, the effective charge and the mean of the equilibrium charge state distribution. The effective charge is extracted from the ion stopping power, which has been introduced by Northcliffe with reference to hydrogen stopping power [4]. The mean of the equilibrium charge state distribution is the average of the projectile charge state distribution at a given energy while in the target $Z_{\mathrm{mean}}(v) = \Sigma_i\{Z_i \cdot n_i(Z_i, v)\}/\Sigma_i n_i$ (n_i stands for the quantity of ions with charge Z_i and energy v of the beam) after equilibrium has occurred. This value typically appears in theoretical expressions but cannot be easily measured [5]. In this Letter, the mean charge of the emerging beam is actually measured: it might slightly differ from the equilibrium since the charge state may have experienced further relaxation processes after exiting the target (e.g., via Auger decay) [6]. Several models have been developed to predict either Z_{mean} (see, for instance, Refs. [7,8]), or the whole evolution of the charge state distribution through *ab initio* models like GLOBAL [9] and ETACHA [10].

In regards to WDM, difficulties arise in calculating the Z_{mean}. Highly charged plasmas at high temperature modify the plasma screening properties and thereby impact ionization, electron capture and recombination rates, and cross sections; moreover, the velocity dependence of those atomic collision processes in strongly ionized matter is not well understood. Hence, the explicit calculation of the mean charge state [11] from first principles is very difficult in dense matter and only quasiempirical models [12] are currently being used to predict the Z_{mean} for light ions passing through WDM.

In this Letter, we report first measurements of the mean charge state of a carbon ion beam, with energy from 0.05 to 0.5 MeV/nucleon (nucl), passing through aluminum WDM. This has been achieved using a new experimental platform for studying interaction of light ions with WDM within a short time scale that avoids any significant change in the WDM condition during the interaction. The results are obtained using two ion beams generated by two independent high intensity short pulse laser beams: one to isochorically heat the solid density sample [13], while the other is used to probe in a single shot the heated sample. The analysis of the data is performed with the aid of two codes: the hydrodynamic code ESTHER [14] to model the target heating process and an extended version of the ETACHA code based on Ref. [10], which is used to predict the mean equilibrium charge state at 300 K over an projectile energy range from 0.1 to 0.5 MeV/nucl.

The experiment was carried out using the ELFIE laser at the Laboratoire pour l'Utilisation des Lasers Intenses (LULI). The experimental setup using two short pulse

beams and three targets is shown in Fig. 1. These types of lasers can create pulsed broadband ion beams of picosecond duration by interacting with flat solid targets via the target normal sheath acceleration (TNSA) mechanism [15,16]. In this process, hot electrons, generated by the short pulse laser, create a sheath field strong enough to ionize and predominantly accelerate hydrocarbons off the target surface.

Laser accelerated ion beams can be used (i) to isochorically heat thick solid-density samples, with negligible hydrodynamic expansion, up to ~20–100 eV [13,17,18] and (ii) as a picosecond-scale probe. Achieving such picosecond-scale heating and probing is significantly harder with ion beams produced in conventional accelerators since the minimum pulse duration produced by accelerator facilities is of the order of nanoseconds. In other words, on this time scale this ion beam is not useful in heating dense targets (or probing them) as hydrodynamic expansion will change the state of the target of interest.

Here, as shown in Fig. 1, the first short pulse beam ($B1$), with 1 J in energy, pulse duration of $\tau = 320$ fs, and intensity of 4×10^{18} W/cm^2 on target, is used to irradiate a very thin Mylar foil (1.5 μm). In this way, similar acceleration fields are expected to develop (thus producing similar ion beam characteristics) on both sides of the Mylar target [19]. One beam is passing through the unheated or proton heated *secondary target*, while the other one is used as a reference. Laser pulse $B1$ is frequency doubled (the fundamental wavelength was 1.057 μm) in order to increase its temporal contrast; a too intense laser pedestal would have damaged the very thin Mylar target inhibiting the symmetrical acceleration. The secondary target is composed of 100 nm aluminum foil. It is isochorically heated to WDM conditions using a picosecond broadband proton beam generated by the second short pulse beam ($B2$). This laser beam is independently compressed with 4 J in energy, pulse duration of $\tau = 320$ fs, and intensity of 1.6×10^{19} W/cm^2 and irradiated a 10 μm thick gold foil to produce the proton beam (see Fig. 1). Its spectrum is fully characterized (in energy and particle flux) by an absolutely calibrated proton spectrometer.

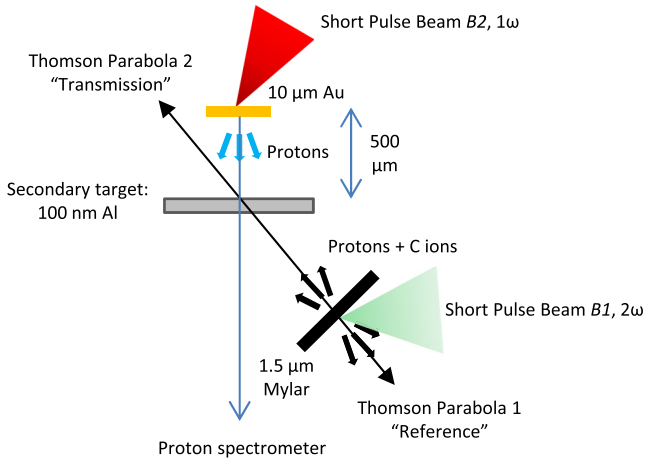

FIG. 1 (color online). Experimental setup.

We have developed a compact platform which allows the measurement of equilibrium charge state distribution on a single shot. Two Thomson parabolas (TP) [20], as shown in Fig. 1, are used to measure the ion beam energy spectrum as well as charge state distribution of the ion beam generated by $B1$, at a distance of 70 cm away from the Mylar target. The TP design that we used has a 100 μm diameter pinhole with a 0.32 T magnetic field inside an iron yoke, a pair of electrodes after the magnets with 6 kV/cm field, and a FujiFilm BAS-TR image plate for the detection. The magnetic field disperses the ions in energy vertically and the electric field separates the various charge states horizontally as a function of charge/mass *ratio*. The simultaneous measurement of the two ion beams, the one from the front side (unperturbed reference beam, TP1) and the other from the back side (the beam that passes through the secondary target of interest, TP2), is necessary in order to compare the two ion spectra on the same shot, thus overcoming shot-to-shot variations [19]. Each TP was absolutely calibrated in energy and efficiency [21], allowing us to retrieve absolute spectra for each ion charge state as a function of ion energy, i.e., to obtain $dN/(dEd\Omega)$ [in part/(MeV · str)].

The symmetry of the "transmitted" and "reference" C ion beams is tested by removing the secondary target. The spectra accelerated forward and backward are not identical in terms of particle numbers and energy cutoff. The maximum energies of the probe beam were 0.2 and 0.6 MeV/nucl, respectively. This is likely due to the fact that the pulse duration employed is not ultrashort, resulting in a stronger deformation of the target front surface than in Ref. [19]. Nevertheless, the charge state fractions of the ion beams accelerated forward and backward are identical at each energy. For the purpose of our experiment, this similarity allows us to use the beam accelerated backward as a reference for the one accelerated forward (the probing ion beam) up to 0.2 MeV/nucl.

The mean charge of both the reference carbon ion beam and the carbon beam after passing through cold (300 K) solid aluminum are shown in Fig. 2 as function of beam energy. What we observe for the reference spectrum is the result of a complex ionization and acceleration process: ionization of the surface ions proceeds mainly by field ionization induced by barrier suppression [22]. Since the ions which are in the target outermost layers will both experience high ionizing fields and high acceleration compared to ions positioned deeper, and for which these fields are partially screened, this process produces the observed correlation at the source between ionization and ion energy: the beam average charge increases with beam energy. On top of this, we observe in Fig. 2 that the mean charge state of ions with energy <0.1 MeV/nucl from

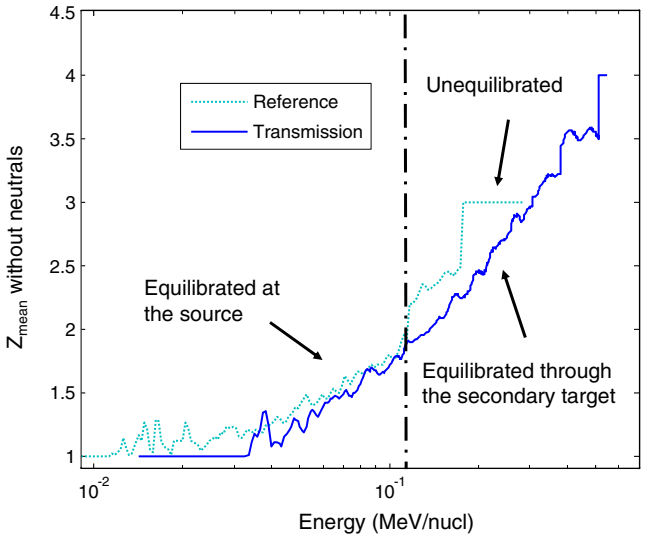

FIG. 2 (color online). Z_{mean} for carbon ions as measured by the "reference" TP1 and "transmission" TP2 after 100 nm of aluminum target at 300 K. The error is ± 0.005 MeV/nucl for the energy and the uncertainty is ± 0.1 for the mean charge.

reference and transmitted beam overlap; this means that the reference carbon beam, for energies <0.1 MeV/nucl, is already equilibrated. There can be two sources for equilibration: (i) equilibration in flight during the ion beam travel to the detector, either with the comoving electrons, or with the background gas, and (ii) interaction with the surrounding plasma at the source since this low energy part of the ion beam (<0.1 MeV/nucl) transits at the source for a longer time in the dense part of the accelerating sheath. As the first can be estimated and the processes are found to be negligible, this suggests that the low energy ions are already at equilibrium when leaving the source target. However, as also shown in Fig. 2, contrary to the low energy portion, the higher energy portion of the spectrum (0.1–0.8 MeV/nucl), is not at equilibrium after leaving the source target; i.e., the "reference" spectrum exhibits higher Z_{mean} than the "through" spectrum. Therefore, we can use this part of the ion beam to characterize the charge altering properties of the secondary target. In summary, a nonequilibrium ion beam is partially dressed after going through the Al target while no change in the charge state distribution occurs if the equilibrium is already reached in the primary ion beam. Finally, we note that, due to the nature of the laser acceleration process, the carbon probe beam, although broadband, is longitudinally laminar [23], i.e., at the time it intercepts the secondary target, the beam is linearly stretched in energy due to the time of flight dispersion.

At this point, it is interesting to compare the equilibrium mean charge of carbon ions in cold aluminium we measured using the through spectrum with some of the semiempirical models which give the effective charge [4,12,24,25], and quasiempirical formulas of Z_{mean} [7,26] or *ab initio* calculations using the extended version of the ETACHA code from which Z_{mean} can be extracted. In Fig. 3(a), we can clearly see that if the effective charge matches the Z_{mean} at high energy, it lies at a higher value when the ion energy decreases as has been discussed for other collision systems in Sigmund's paper [3].

In Fig. 3(b), we compare the data obtained with a cold target in a single shot with the extended version of the ETACHA code. The code can predict the population of projectile electronic states, $n\ell$ up to $n = 3$, by solving a set of coupled differential rate equations. Ion-atom cross sections for capture, ionization, and excitation processes are used and radiative and Auger deexcitations are included as well. In its first version (as described in Ref. [10]), the validity domain was limited to high projectile energy, but it has been improved recently by using nonperturbative theories to describe the atomic collision processes that extend its application domain towards lower energy, i.e., down to 0.1 MeV/nucl relevant for the present case of carbon on aluminum. In Fig. 3(b), we also reported Shima's empirical curve [26] based on measurements from

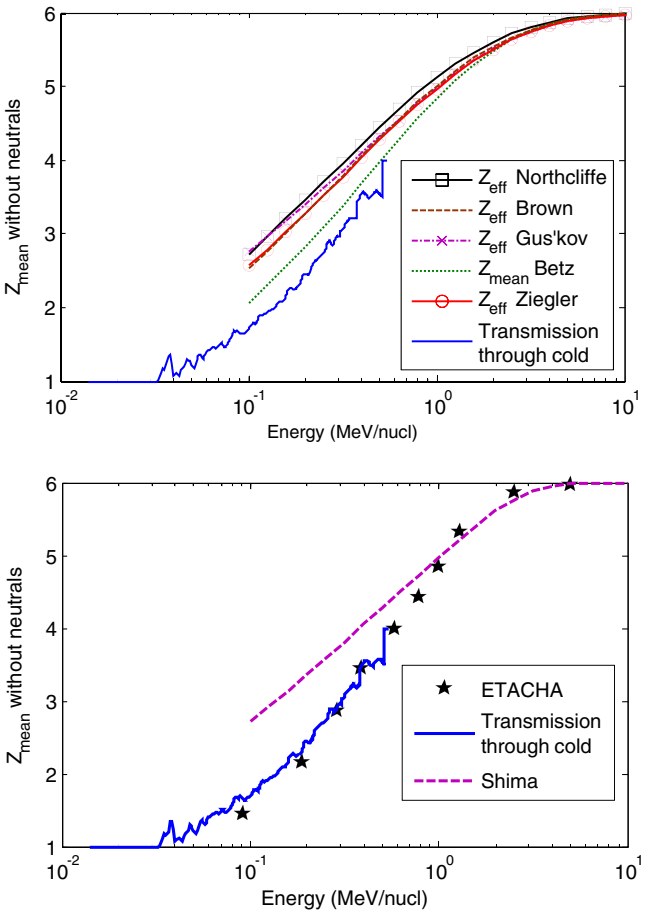

FIG. 3 (color online). Comparison between Z_{mean} from our experiment with (a) the *effective* charge from Refs. [4,12,24,25] and Z_{mean} from Betz [7]; (b) Z_{mean} from Shima [26] and from ETACHA.

conventional accelerator devices compiled in Ref. [27]. Since our experimental platform did not include diagnostics for the neutrals, it should be noted that all the Z_{mean} values reported here (from code or data) are given without including the neutrals. However, according to the ETACHA code, this only affects the calculation below 0.1 MeV/nucl.

From Fig. 3(b), one can see that our data obtained with the cold Al target are fully consistent with the ETACHA calculations that has been found to be entirely reliable when compared to charge state distributions obtained with conventional accelerator devices for collision systems similar to the one currently studied here. On the other hand, our experimental data lie at lower mean charge state values when compared with the commonly used empirical formula given by Shima [8] by, at most, 15%. This was not *a priori* unexpected since others, for higher Z ions, have already shown that the Shima's formula overestimates the mean charge [28]. Since the error bar in the calibration of our detector is of ± 0.005 MeV/nucl, the agreement between the ETACHA code and our data for cold target positively assesses our new experimental platform.

Therefore, we repeated the measurements through proton-heated material. The plasma conditions of the proton heated secondary target are calculated using the 1D Lagrangian hydrodynamics code ESTHER [14]. Using the measured heating proton parameters, this procedure has been well-assessed in previous proton heating experiments [13,27] with the same range of densities and temperatures.

The plasma characteristics of the secondary target heated by protons over the course of several tens of picoseconds are shown in Fig. 4. We can see that there exists a window of ~100 ps where the plasma is in the desired regime of WDM. By adjusting the delay between $B1$ and $B2$, and accounting for the time of flight of the probe ion beam, a desired interval of carbon ion energies can probe the WDM conditions (an example for a particular delay is shown on the top axis of Fig. 4). In this experiment, we aimed to employ ion energies below 1 MeV/nucl to probe the WDM conditions since it is for such energies [12] that we can expect Z_{mean} to be modified compared to when passing through cold matter.

The experimental mean charge state of the ion probe beam passing through heated plasma is presented in Fig. 5. The carbon ion probe beam arrived here at the secondary target such that ions with energies 0.41–0.53 MeV/nucl passed through heated plasma, as shown in Fig. 4. When compared to results of unheated aluminum, we can conclude that heating aluminum to 1 eV does not significantly affect the equilibration of states of the ion beam as the curves in Fig. 5 for heated and unheated aluminum are almost overlapping. Similar results were obtained when we changed the delay between $B1$ and $B2$ so that different energy intervals of the carbon ion beam-probe can be explored: namely for 0.09–0.1 and 0.045–0.05 MeV/nucl passing through the aluminum target while in the WDM conditions shown in Fig. 4. These results may not be surprising: although the probe beam passes through WDM, the aluminum foil is heated to 1 eV, which, regarding the perturbation induced to atomic collision processes inside the material, does not correspond to a truely ionized medium on the average.

In conclusion, we have demonstrated that we can reproduce well, with our experimental setup, the data obtained in cold matter with accelerators on a single shot. Accordingly, a very good agreement is found with the results of the ETACHA code in its recent version.

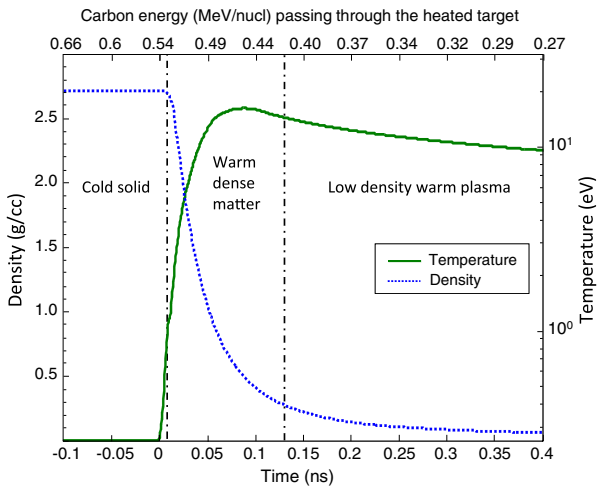

FIG. 4 (color online). Density and temperature of the heated aluminum target as simulated by ESTHER using the measured heating proton parameters.

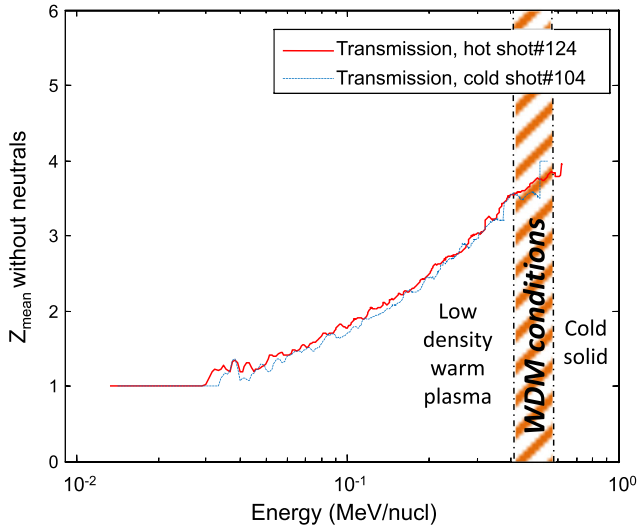

FIG. 5 (color online). Z_{mean} of the carbon ion beam as measured by the TP2 through 100 nm of aluminum *cold* or *heated* to 1 eV. The shot was timed such that the ion beam with energy 0.41–0.53 MeV/nucl came to equilibrium through the warm dense aluminum plasma (see Fig. 4).

Furthermore, we have also demonstrated for the first time that measurements of the mean charge state of an ion beam passing in WDM under well controlled conditions can be realized. We have shown that plasma effects in WDM heated up to 1 eV do not significantly impact the mean charge of a 0.04–0.5 MeV/nucl carbon beam passing through aluminum. Such measurements open up an untouched regime where we can test various theoretical predictions. Next steps will be to perform similar measurements for other ions and certainly at higher temperature in WDM. Recent achievements of ultrafast isochoric heating of solids up to 100 eV using x-ray free-electron laser beams [29] offer interesting perspectives in this respect.

We acknowledge the support of the LULI technical team. We thank Michel Boustie and Laurent Berthe for use of their equipment. This work has been partly performed within the Labex PLAS@PAR, funded by the ANR-11-IDEX-004-02 contract. This work was supported by the National Science Foundation, Grant No. 1064468, LASERLAB Europe, Grant No. 001528, EPSRC Grants No. EP/E035728/1 (LIBRA consortium) and No. EP/I029206/1, and the ULIMAC grant from the Triangle de la Physique RTRA network. Authors M. C., C. P., T. T., and O. W. acknowledge the support received during this work by the DFG Transregio SFB-TR 18 and GRK 1203 programs. Author M. B. acknowledges funding from projects ELI (Grant No. CZ.1.05/1.1.00/483/02.0061) and OPVK 3 (Grant No. CZ.1.07/2.3.00/20.0279).

*julien.fuchs@polytechnique.fr

[1] R. W. Lee *et al.*, J. Opt. Soc. Am. B **20**, 770 (2003).
[2] C.-K Li and R. D. Petrasso, Phys. Rev. Lett. **70**, 3059 (1993).
[3] P. Sigmund and A. Schinner, Nucl. Instrum. Methods Phys. Res., Sect. B **174**, 535 (2001).
[4] L. C. Northcliffe, Phys. Rev. **120**, 1744 (1960).
[5] S. Della-Negra, Y. LeBeyec, B. Monart, K. Standing, and K. Wien, Phys. Rev. Lett. **58**, 17 (1987).
[6] A. Brunelle, S. Della-Negra, J. Depauw, H. Joret, Y. Le Beyec, and K. Wien, Nucl. Instrum. Methods Phys. Res., Sect. B **43**, 484 (1989).
[7] H. D. Betz and L. Grodzins, Phys. Rev. Lett. **25**, 211 (1970).
[8] K. Shima, N. Kuno, and M. Yamanouchi, Phys. Rev. A **40**, 3557 (1989).
[9] C. Scheidenberger, Th. Stöhlker, W. E. Meyerhof, H. Geissel, P. H. Mokler, and B. Blank, Nucl. Instrum. Methods Phys. Res., Sect. B **142**, 441 (1998).
[10] J. P. Rozet, C. Stephan, and D. Vernhet, Nucl. Instrum. Methods Phys. Res., Sect. B **107**, 67 (1996).
[11] H. D. Betz, Rev. Mod. Phys. **44**, 465 (1972).
[12] S. Y. Gus'kov, N. V. Zmitrenko, D. V. Il'in, A. A. Levkovskii, V. B. Rozanov, and V. E. Sherman, Plasma Phys. Rep. **35**, 709 (2009).
[13] A. Mancic *et al.*, High Energy Density Phys. **6**, 21 (2010).
[14] J. P. Colombier, P. Combis, F. Bonneau, R. Le Harzic, and E. Audouard, Phys. Rev. B **71**, 165406 (2005).
[15] G. Guethlein, D. Price, J. Swenson, M. Glinsky, R. Shepherd, and R. Stewart, AIP Conf. Proc. **318**, 77 (1994).
[16] S. C. Wilks, A. B. Langdon, T. E. Cowan, M. Roth, M. Singh, S. Hatchett, M. H. Key, D. Pennington, A. MacKinnon, and R. A. Snavely, Phys. Plasmas **8**, 542 (2001).
[17] G. Dyer *et al.*, Phys. Rev. Lett. **101**, 015002 (2008).
[18] R. A. Snavely *et al.*, Phys. Plasmas **14**, 092703 (2007).
[19] T. Ceccotti, A. Lévy, H. Popescu, F. Réau, P. D'Oliveira, P. Monot, J. Geindre, E. Lefebvre, and Ph. Martin, Phys. Rev. Lett. **99**, 185002 (2007).
[20] C. G. Freeman *et al.*, Rev. Sci. Instrum. **82**, 073301 (2011).
[21] D. Doria *et al.*, Central Laser Facility, Rutherford Appleton Laboratory (UK), Annual Report No. 2009/10, p. 78.
[22] M. Hegelich *et al.*, Phys. Rev. Lett. **89**, 085002 (2002).
[23] H. Ruhl, T. Cowan, and J. Fuchs, Phys. Plasmas **11**, L17 (2004).
[24] N. V. Novikov and Ya. A. Teplova, J. Phys. Conf. Ser. **194**, 082032 (2009).
[25] M. D. Brown and C. D. Moak, Phys. Rev. B **6**, 90 (1972).
[26] K. Shima, T. Ishihara, and T. Mikumo, Nucl. Instrum. Methods **200**, 605 (1982).
[27] F. Besenbacher, J. U. Andersen, and E. Bonderup, Nucl. Instrum. Methods **168**, 1 (1980).
[28] R. N. Sagaidak and A. V. Yeremin, Nucl. Instrum. Methods Phys. Res., Sect. B **93**, 103 (1994).
[29] S. M. Vinko *et al.*, Nature (London) **482**, 59 (2012).